

High-Temperature Free Radical Copolymerization of Styrene and Butyl Methacrylate with Depropagation and Penultimate Kinetic Effects

Deheng Li, Ning Li, and Robin A. Hutchinson*

Department of Chemical Engineering, Dupuis Hall, Queen's University, Kingston, Ontario K7L 3N6, Canada

Received February 24, 2006; Revised Manuscript Received May 2, 2006

ABSTRACT: Copolymers of methacrylate and styrene, the main components of many solvent-based automotive coating formulations, are produced under higher temperature starved-feed conditions in order to reduce the solvent level while controlling polymer composition. Under these conditions methacrylate depropagation has a significant impact on polymer molecular weights and free monomer concentrations in the reactor. Meanwhile, a strong penultimate effect has been observed for this binary system at lower temperatures, also affecting the polymerization rate. In this work, the combined effect of depropagation and penultimate copolymerization kinetics is investigated. The copolymer-averaged propagation rate coefficient for butyl methacrylate and styrene is determined as a function of monomer composition using pulsed-laser polymerization over a range of temperatures. A clear penultimate effect is seen even at the elevated temperatures at which depropagation is important. Radical and monomer reactivity ratios show a negligible temperature dependency between 50 and 150 °C. The Lowry case 1 representation adequately describes the effect of methacrylate depropagation over the range of conditions examined.

Introduction

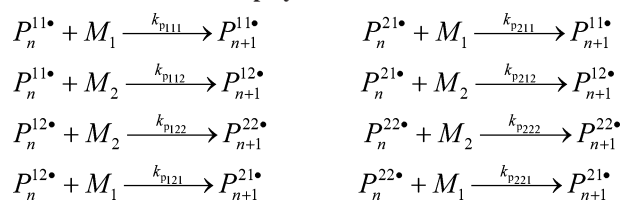
The synthesis of multicomponent polymers remains of significant economic importance due to the ability to produce materials with a great diversity of properties compared to those of homopolymers. Copolymers of methacrylate and styrene are used as binder resins in automotive coatings, providing excellent protection against chemical and mechanical attack. These polymers are produced at higher temperature (>120 °C) using a semibatch starved feed policy to control copolymer composition and solution viscosity with reduced solvent content in the system.¹ While often studied at lower temperatures, many of the basic copolymerization kinetic coefficients have not been measured under these high-temperature conditions. This study, which also examines the effect of depropagation in the system, rectifies this situation.

Mayo and Lewis² first examined the free radical copolymerization of styrene (ST) and methyl methacrylate (MMA) to demonstrate that the composition of a copolymer can be expressed as a function of the initial monomer concentrations and reactivity ratios ($r_i = k_{pi}/k_{pji}$, where k_{pji} is the rate coefficient for addition of monomer j to radical i) according to the terminal model, in which radical reactivity depends only on the identity of the terminal unit on the growing chain.

$$F_1^{\text{inst}} = \frac{r_1 f_1^2 + f_1 f_2}{r_1 f_1^2 + 2f_1 f_2 + r_2 f_2^2} \quad (1)$$

In eq 1, f_i is the mole fraction of monomer i (e.g., $f_1 = [M_1]/[M_1] + [M_2]$), and F_1^{inst} is the mole fraction of repeat unit 1 in the polymer at that instant. The copolymer-averaged propagation

Scheme 1. Penultimate Propagation Kinetic Scheme for Binary Copolymerization^a



^a Addition of monomer k (M_k) to a growing radical of length n with terminal radical unit j and penultimate unit i ($P_n^{ij\bullet}$) is described by rate coefficient k_{pijk} .

rate coefficient derived by the terminal model is expressed by eq 2.

$$k_{p,\text{copo}} = \frac{r_1 f_1^2 + 2f_1 f_2 + r_2 f_2^2}{[r_1 f_1/k_{p11}] + [r_2 f_2/k_{p22}]} \quad (2)$$

Thus, the polymer composition is only a function of reactivity ratios while the average propagation rate coefficient is also a function of the individual propagation rate coefficients.

To test the general validity of the terminal model, Fukuda et al.³ measured $k_{p,\text{copo}}$ for MMA/ST copolymerization at 40 °C as a function of composition using the rotating-sector technique. The copolymer composition conformed to the terminal model, whereas the propagation rate constant was significantly over-predicted by eq 2. The same result was found by Davis and O'Driscoll⁴ using pulsed laser polymerization (PLP) techniques, thus confirming the postulate that radical stabilization energy is affected by the identity of the penultimate unit. The basis of the penultimate model is described in Scheme 1.

$P_n^{ij\bullet}$ represents a growing chain of length n with terminal radical unit j and penultimate unit i . Addition of M_k to the radical is described by rate coefficient k_{pijk} . For a two-monomer system, the model has eight possible propagation reactions, as shown in Scheme 1. As found by Fukuda and co-workers³ and

* Corresponding author. E-mail: robin.hutchinson@chee.queensu.ca.

Table 1. Styrene (ST)/Butyl Methacrylate (BMA) Monomer and Radical Reactivity Ratios from the Literature

monomer reactivity ratios				radical reactivity ratios			
<i>T</i> (°C)	<i>r</i> _{ST}	<i>r</i> _{BMA}	source	<i>T</i> (°C)	<i>s</i> _{ST}	<i>s</i> _{BMA}	source
25	0.72	0.45	8	25	0.56	0.63	8
50	0.85	0.18	9	55	0.50	0.67	8
55	0.72	0.45	8				
	0.56	0.31	10				
	0.52	0.47	11				
	0.74	0.59	12				
80	0.87	0.58	13				

subsequent studies,⁴ polymer composition is well represented by the terminal model of eq 1, as the penultimate unit does not affect the selectivity of the radical. Thus, only a single pair of monomer reactivity ratios ($r_1 = k_{p111}/k_{p112} = k_{p211}/k_{p212}$; $r_2 = k_{p222}/k_{p221} = k_{p122}/k_{p121}$) is required. However, the penultimate unit affects the radical reactivity as captured by the radical reactivity ratios ($s_1 = k_{p211}/k_{p111}$; $s_2 = k_{p122}/k_{p222}$), which differ significantly from unity. For this case, called the implicit penultimate unit effect (IPUE) model, the copolymer-averaged propagation rate constant is represented by

$$k_{p, \text{copo}} = \frac{r_1 f_1^2 + 2f_1 f_2 + r_2 f_2^2}{[r_1 f_1 / \bar{k}_{11}] + [r_2 f_2 / \bar{k}_{22}]} \quad (3)$$

where \bar{k}_{ii} are functions of monomer composition according to eq 4.

$$\bar{k}_{11} = \frac{k_{p111}[r_1 f_1 + f_2]}{r_1 f_1 + [f_2/s_1]} \quad \bar{k}_{22} = \frac{k_{p222}[r_2 f_2 + f_1]}{r_2 f_2 + [f_1/s_2]} \quad (4)$$

These earlier studies were conducted at temperatures less than 60 °C and generally at a single temperature. To study the effect of temperature on the penultimate kinetics, Coote et al. performed PLP experiments on the MMA/ST binary system over the temperature range 18–57 °C.^{5,6} This careful study concluded that there was no significant temperature dependence of the monomer reactivity ratios (*r* values) within experimental uncertainty. In addition, while penultimate effects were observed over the complete 40 °C temperature range, there was no significant temperature dependence of the radical reactivity ratios (*s* values). Thus, it could not be concluded whether the penultimate effect was mainly enthalpic or entropic in nature.

Much of the data in the literature examines styrene copolymerization with MMA. The current study focuses on styrene copolymerization with *n*-butyl methacrylate (BMA), to follow our previous copolymerization study of BMA with *n*-butyl acrylate.⁷ While the amount of available data for ST/BMA is reduced compared to ST/MMA, the systems are very similar. As summarized in Table 1, both monomer reactivity ratios are smaller than unity with *r*_{ST} larger than *r*_{BMA}. Both *s* values are also less than unity,⁸ reflecting the fact that the penultimate effect decreases the polymerization rate compared to terminal model predictions. As for other styrene/methacrylate systems, there is significant uncertainty in the *s*_{BMA} estimate, since the shape of the $k_{p, \text{copo}}$ vs f_{ST} curve is largely controlled by the value of *s*_{ST}.^{6,8} To the best of our knowledge, penultimate kinetics have not been studied for ST/BMA, nor for any other copolymerization system, at temperatures above 60 °C.

At elevated temperatures (>120 °C), depropagation can also affect the chain growth kinetics of methacrylates. The reversible behavior of propagation for methacrylates was first discovered by Bywater¹⁴ in MMA solution polymerization at elevated temperatures. An equilibrium concentration of monomer is

attained at each temperature regardless of the initial monomer concentration. Since then, the mechanism has been studied widely. Hutchinson et al.¹⁵ investigated depropagation of several methacrylates at higher temperatures using PLP, providing further strong evidence of the increasing importance of depropagation with increasing temperature and decreasing monomer concentration.

Two main types of models have been proposed for depropagation in copolymerization systems by Lowry¹⁶ and Wittmer.¹⁷ Lowry's approach assumes that only one of the monomers is sufficiently close to its ceiling temperature to have significant depropagation. In Lowry case 1, depropagation only occurs when the radical contains the depropagating monomer in both the terminal and penultimate positions. The resulting derivation, an extension of the steady-state kinetic solution for polymer composition in a nondepropagating copolymerization, has been successfully applied to many binary systems including methacrylate and acrylate copolymerization.⁷ Wittmer's treatment considers the more general case where both monomers can depropagate such that all the propagation steps are reversible. Both models have been extensively used over the past decades, including an extension of Lowry's model to examine the effect of depropagation on the copolymer-averaged propagation rate coefficient, $k_{p, \text{copo}}$.¹⁸ All of these previous studies, however, examine depropagation in combination with terminal propagation kinetics; penultimate effects on chain growth are not considered. Recently we have developed a system of equations to describe instantaneous polymer composition and $k_{p, \text{copo}}$ for a copolymerization system under the influence of both depropagation and penultimate chain growth kinetics.¹⁹ Simulations show that when reversible reactions are involved, the implicit penultimate unit effect not only decreases $k_{p, \text{copo}}$ but also has an impact on copolymer composition.

In this work, PLP experiments are performed to determine $k_{p, \text{copo}}$ for the ST/BMA binary system at higher temperatures. The data are combined with polymer composition measurements from low conversion experiments and used to estimate monomer and radical reactivity ratios at temperatures between 50 and 150 °C. In addition, high temperature, low monomer concentration experiments are run to study the influence of depropagation. The data are required in order to better understand and model the kinetics of these systems under industrially relevant conditions.¹

Experimental Section

BMA with 10–55 ppm of methyl ether hydroquinone, and styrene inhibited with 10–15 ppm of 4-*tert*-butylcatechol were purchased from Sigma Aldrich at 99% purity and used as received. The photoinitiator DMPA (2,2-dimethoxy-2-phenylacetophenone, 99% purity) and *n*-octyl acetate solvent with boiling point 211 °C were also purchased from Sigma Aldrich and used as received.

Low-conversion polymerizations were conducted in a pulsed laser setup consisting of a Spectra-Physics Quanta-Ray 100 Hz Nd:YAG laser that is capable of producing a 355 nm laser pulse of duration 7–10 ns and energy of 1–50 mJ per pulse. The laser beam is reflected twice (180°) to shine into a Hellma QS165 0.8 mL jacketed optical sample cell used as the PLP reactor. A digital delay generator (DDG, Stanford Instruments) is attached to the laser in order to regulate the pulse output repetition rate at a value between 10 and 100 Hz. Monomer mixtures in bulk or octyl acetate solution with 1–10 mmol L⁻¹ DMPA photoinitiator were added to the cylindrical quartz cell and exposed to laser energy, with temperature controlled by a circulating oil bath. Experiments were run in the temperature range of 50–180 °C, with styrene fraction in the monomer mixture varied between 0 and 100%. Monomer conversions were usually below 5% to avoid significant composition drift; a few of the highest

Table 2. Copolymer Composition Data for Low-Conversion Styrene (ST)/Butyl Methacrylate (BMA) Copolymerization: Mole Fraction BMA in Copolymer (F_{BMA}) vs Mole Fraction BMA in Monomer Mixture (f_{BMA})^a

bulk copolymerization				solution copolymerization			
T (°C)	f_{BMA}	F_{BMA}	conv (%)	T (°C)	f_{BMA}	F_{BMA}	conv (%)
50	0.092	0.139	2.6	70	0.152	0.204	0.90
50	0.282	0.315	2.9	70	0.323	0.365	0.49
50	0.547	0.500	4.0	70	0.517	0.496	0.21
50	0.884	0.798	5.1	70	0.741	0.646	0.25
70	0.192	0.223	2.7	140	0.931	0.846	4.4
70	0.417	0.397	3.0	140	0.865	0.779	2.1
70	0.682	0.599	3.2	140	0.802	0.722	2.1
100	0.152	0.188	4.7	140	0.741	0.665	2.4
100	0.323	0.341	4.1	140	0.417	0.431	2.2
100	0.517	0.463	4.8	140	0.192	0.242	2.1
140	0.931	0.887	6.5	150	0.802	0.710	5.7
140	0.865	0.759	6.8	150	0.417	0.426	8.1
140	0.802	0.736	8.7	150	0.192	0.241	6.3
140	0.741	0.671	8.3				

^aSolution experiments were performed in 50 vol % *n*-octyl acetate solvent.

temperature experiments went to slightly higher conversion. For example, 0.03 g (0.12 mmol) of DMPA was dissolved in a mixture of 4 mL (24.8 mmol) of BMA, 1 mL (8.6 mmol) of ST, and 50 mL of *n*-octyl acetate solvent. 4 mL of this solution was transferred to the PLP sample cell, which was heated to 170 °C and pulsed for 4 min in the laser setup at a repetition rate of 100 Hz. Following the isolation procedure described below, 10.6 mg of polymer was obtained, a conversion of 2.3%.

The pulsed laser setup was used to produce polymer for composition analysis by proton NMR. The resulting samples were precipitated in methanol, redissolved in dichloromethane and reprecipitated twice, and dried in a vacuum oven at 60 °C. The polymer was then dissolved in *d*-chloroform for ¹H NMR analysis conducted at room temperature on a 400 MHz Bruker instrument. The copolymer shows chemical shifts from the phenyl protons in the region of 6.6–7.3 ppm and from the methyleneoxy (–OCH₂–) protons of BMA units in the region 2.7–4.1 ppm. The remainder of the spectra contains signals for protons in the copolymer methine, methylene, and methyl groups.²⁰ Copolymer composition was estimated from proton NMR via two methodologies. For the first, the peak area from the phenyl protons is taken as 5ST, while the remainder of the spectrum is integrated to yield the remaining (3ST + 14BMA) protons. This ratio is used to calculate the molar percentage of BMA units in the copolymer, BMA/(BMA + ST).²⁰ For the second, the mole fraction of BMA in the polymer is calculated according to $F_1 = 5A_1/(5A_1 + 2A_2)$, where A_1 and A_2 are the peak areas of the methyleneoxy and phenyl protons, respectively.¹³ The polymer compositions estimated by the two methods agreed well with reported values determined by the method employing the entire spectra.

The PLP apparatus was also used to produce polymers for determination of $k_{p,\text{copo}}$ from analysis of the polymer molecular weight distribution (MWD) measured by size exclusion chromatography (SEC). Molecular weight distributions were measured with a Waters 2960 separation module connected to a Waters 410 differential refractometer (DRI) and a Wyatt Instruments Dawn EOS 690 nm laser photometer multiangle light scattering (LS) detector. THF was used to carry the polymer at a flow rate of 1 mL/min through the four Styragel columns (HR 0.5, 1, 3, 4) maintained at 35 °C. The DRI detector was calibrated by 10 molecular weight polystyrene standards with narrow polydispersities (870–355000 Da). The LS detector was calibrated by toluene as recommended by the manufacturer. The refractive index (dn/dc) of the polymer in THF is required to process the data from the LS detector. A Wyatt Optilab DSP refractometer was used to measure these values for several BMA/ST copolymer samples. Before running the samples, the instrument was first calibrated with sodium chloride. Six samples of 1–10 mg mL^{−1} were prepared in THF for each polymer and injected sequentially to construct a curve with slope dn/dc .

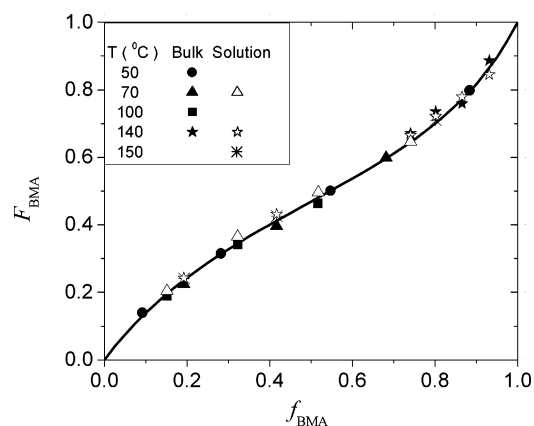


Figure 1. Copolymer composition data for low-conversion styrene (ST)/butyl methacrylate (BMA) copolymerization: mole fraction BMA in copolymer (F_{BMA}) vs mole fraction BMA in monomer mixture (f_{BMA}). Solution experiments were performed in 50 vol % *n*-octyl acetate solvent. Curve shows the best fit of the Mayo–Lewis equation to the data, with $r_{\text{BMA}} = 0.42$ and $r_{\text{ST}} = 0.61$.

Results and Discussion

Monomer Reactivity Ratios. Because of the uncertain temperature dependencies of r values and the lack of composition data at higher temperatures, low-conversion experiments were carried out in the temperature range of 50–150 °C by copolymerizing ST and BMA in bulk as well as in 50 vol % octyl acetate. Table 2 lists the composition data for the monomer mixtures and corresponding copolymers used to construct the Mayo–Lewis plot shown as Figure 1. Within experimental uncertainty (estimated as ± 0.03 based upon a comparison of the two techniques to measure composition from the proton NMR spectra), the polymer composition does not show a discernible dependence on temperature. In addition, the bulk and solution values are also within the limits of experimental error, even at 140 °C. Thus, no depropagation effect is observed at these conditions with high total monomer concentration ($[M]_{\text{tot}} > 4 \text{ mol L}^{-1}$). The effect of depropagation on BMA/ST copolymerization at lower $[M]_{\text{tot}}$ is examined in the latter part of this work.

To ensure the parameter estimates are not affected by depropagation, only the data collected between 50 and 100 °C have been used to estimate the monomer reactivity ratios using nonlinear regression. As shown in Figure 1, the copolymer composition data are well represented by the terminal propagation model. The values of $r_{\text{BMA}} = 0.42 \pm 0.03$ and $r_{\text{ST}} = 0.61 \pm 0.03$ are in reasonable agreement with the literature data of

Table 3. Constants Required for Calculation of $k_{p,copo}$ from PLP/SEC Data

monomer	monomer density ρ (g mL ⁻¹) = $\rho_0 - bT/^\circ\text{C}$	polymer dn/dc (mL g ⁻¹)	polymer Mark–Houwink parameters		
			K (dL g ⁻¹)	a	ref
styrene	0.9193 – 0.0006657 ²⁵	0.180 ²⁶	1.14×10^{-4}	0.716	27
butyl methacrylate	0.91454 – 0.0009647 ²⁸	0.080 ²⁶	1.48×10^{-4}	0.664	27

Table 1. As shown in Figure 1, these monomer reactivity ratios provide a good representation of polymer composition over the complete temperature range for both bulk and solution systems. Thus, they will be used in the subsequent analyses of penultimate and depropagation kinetics.

Penultimate Kinetics. Pulsed laser experiments were carried out between 70 and 140 °C for BMA and ST monomer mixtures of varying composition containing 3–10 mmol L⁻¹ DMPA photoinitiator. Each laser flash generates a burst of radicals in the reaction mixture, with a sufficient fraction of these radicals propagating up to a length L_0 corresponding to a chain lifetime equal to the time between pulses, t_0 . There is a high probability that these chains will be terminated by the new radicals from the next flash, such that a distinctive peak is formed in the polymer molecular weight distribution corresponding to the chain length L_0 and directly proportional to the propagation rate coefficient according to the relation

$$L_0 = k_p[M]t_0 \quad (5)$$

Given total monomer concentration $[M]$ and flash interval t_0 , the propagation rate constant k_p can be determined. In the case of copolymerization, k_p is the copolymer-averaged propagation rate coefficient $k_{p,copo}$.

The accuracy of k_p values measured by the PLP-SEC technique relies upon determination of the characteristic chain length L_0 from the polymer MWD, estimated from the point of inflection on the low molar mass side of the peak of the MWD.^{21,22} In this work, all k_p values are estimated from SEC weight-log MWDs, with derivative plots calculated using MWDs from both the RI and LS detectors. Molecular weight values for the first, second, and (sometimes) tertiary inflection points are recorded from the derivative plots, and the k_p values calculated from the first inflection point according to a rearranged form of eq 5:

$$k_p = \frac{MW_0}{1000\rho t_0} \quad (6)$$

where MW_0 is the polymer molecular weight at the first inflection point and ρ (g mL⁻¹) is the density of the comonomer mixture calculated assuming volume additivity.

As discussed in previous literature,^{5,23} a difficulty in estimating $k_{p,copo}$ using PLP is SEC calibration for the copolymer system. Coote et al.⁵ found that MWDs for MMA/ST copolymer could be estimated from DRI data as a mass-weighted average of the two homopolymer calibrations. The same approach is used here. The LS detector provides an additional measure of polymer MWD, providing the differential index of refraction, dn/dc , is known. Following previous practice,^{7,23} this value is estimated using a weighted average of the known homopolymer values. The validity of this assumption was verified by measuring dn/dc values of several copolymer samples using a Wyatt Optilab rEX refractometer operating at the same light wavelength (690 nm) and temperature (35 °C) as the LS detector, as detailed elsewhere.²⁴ The set of constants required to estimate $k_{p,copo}$ from the polymer MWDs is summarized in Table 3.

The data set obtained at 70 °C, the lowest temperature examined, is summarized in Table 4. For each sample, there

Table 4. Styrene (ST)/Butyl Methacrylate (BMA) PLP Experiments at 70 °C^a

f_{BMA} (mol frac)	F_{BMA}^b (mol frac)	repetition rate (Hz)	conv (%)	$k_{p,copo}$ (L mol ⁻¹ s ⁻¹)	
				DRI	LS
0.000	0.000	20	2.4	484	520
0.000	0.000	20	2.3	483	516
0.192	0.235	20	2.7	463	464
0.192	0.235	20	2.4	470	467
0.416	0.411	20	3.0	495	481
0.416	0.411	20	2.4	492	477
0.681	0.596	20	3.2	609	602
0.681	0.596	20	2.5	604	558
1.000	1.000	20	12.5	1105	1132
1.000	1.000	20	10.0	1075	1110
0.000	0.000	50	1.7	535	550
0.000	0.000	50	2.3	535	550
0.192	0.235	50	2.3	494	475
0.192	0.235	50	2.0	498	478
0.416	0.411	50	2.0	572	546
0.416	0.411	50	2.0	536	539
0.681	0.596	50	1.8	678	672
0.681	0.596	50	1.7	692	667
1.000	1.000	50	3.6	1409	1409
1.000	1.000	50	3.2	1387	1377

^a All experiments with bulk monomer containing 6–7 mmol L⁻¹ DMPA photoinitiator and laser energy of 3–10 mJ per pulse. ^b Calculated from f_{BMA} with $r_{ST} = 0.61$ and $r_{BMA} = 0.42$.

are estimates of $k_{p,copo}$ from both DRI and LS detectors. The MWDs and derivative plots from the samples pulsed at 20 Hz are shown as Figure 2. Clear primary and secondary inflection points are observed, with the position of the secondary inflection point at twice the value of the primary, an important consistency check for PLP analysis.^{21,22} The distributions shift to higher MW as the fraction of BMA in the system increases, with the biggest shift seen for 75 and 100 vol % BMA in the monomer mixture. This shift reflects the increasing $k_{p,copo}$ with BMA content summarized in Table 4. Values of $k_{p,copo}$ determined from DRI and LS are in good agreement (within 10%) for each sample, validating the assumptions and parameters used for SEC analysis.

Figure 3 plots $k_{p,copo}$ as a function of monomer composition for the 70 °C data. The k_p estimates determined at 50 Hz are about 10% higher than the estimates obtained at 20 Hz at the same temperature, with the difference slightly greater for BMA homopolymerization. It is interesting to compare the homopolymer results to values calculated according to the best-fit Arrhenius expressions to IUPAC benchmark data sets for styrene²¹

$$k_{p,ST} (\text{L mol}^{-1} \text{s}^{-1}) = 10^{7.630} \exp\left(\frac{-32.51 \text{ kJ mol}^{-1}}{RT}\right) \quad (7)$$

and BMA.²²

$$k_{p,BMA} (\text{L mol}^{-1} \text{s}^{-1}) = 10^{6.58} \exp\left(\frac{-22.9 \text{ kJ mol}^{-1}}{RT}\right) \quad (8)$$

From these equations, the IUPAC k_p values for styrene and BMA at 70 °C are 480 and 1241 L mol⁻¹ s⁻¹, respectively. This BMA value is about midway between the 20 Hz (1075–1132 L mol⁻¹ s⁻¹) and 50 Hz (1377–1409 L mol⁻¹ s⁻¹) values

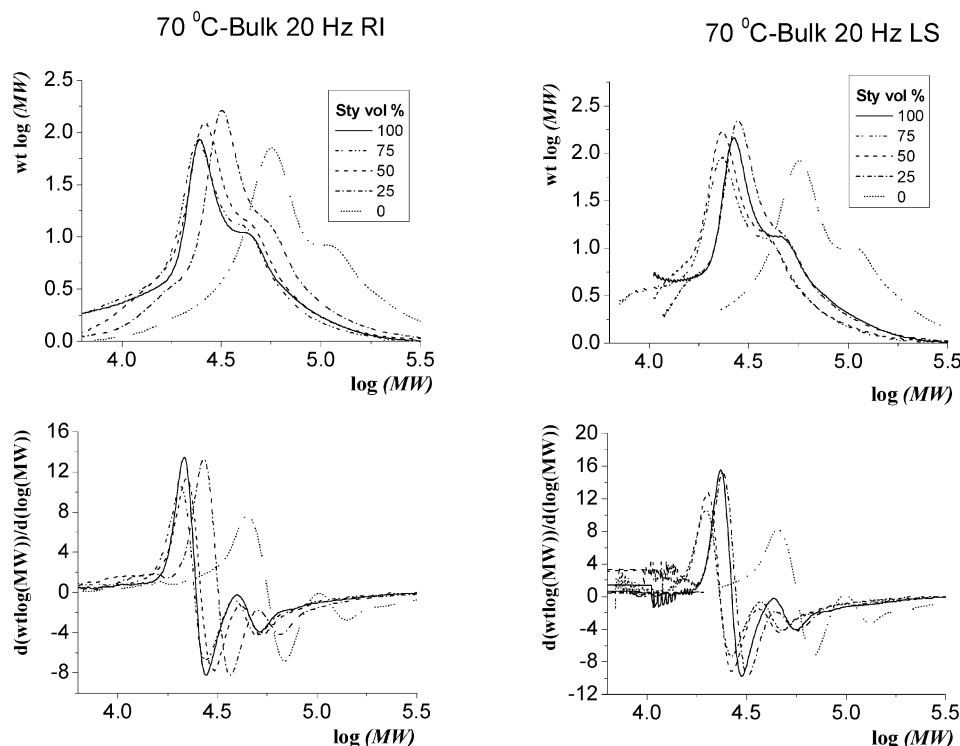


Figure 2. Molecular weight distributions (top) and corresponding derivative (bottom) plots obtained for styrene/butyl methacrylate copolymer produced by PLP at 70 °C and 20 Hz, as measured by refractive index (left-hand side) and light scattering (right-hand side) detectors.

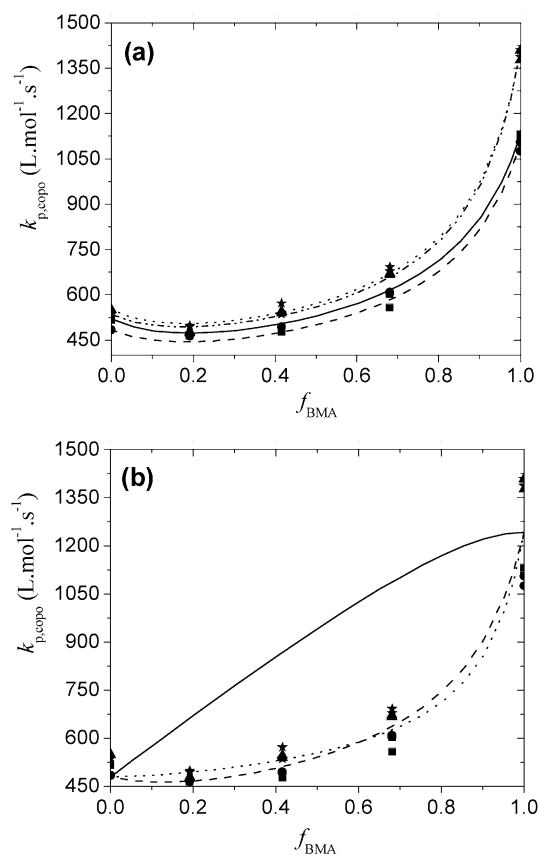


Figure 3. Experimental $k_{p,copo}$ data vs butyl methacrylate monomer mole fraction obtained by PLP/SEC at 70 °C. (a) Individual data sets (points) and corresponding penultimate model fits (lines): 20 Hz/DRI (■, —); 20 Hz/LS (●, —); 50 Hz/DRI (▲, —·), and 50 Hz/LS (★, ···). (b) Overall fit to combined data set by the penultimate model (—), prediction of the terminal model (---), and penultimate model fit using r and s values from Davis et al.⁸ (···).

obtained here. There is a debate as to whether k_p shows a small chain-length dependence, based on a small but significant increase in values as pulse repetition rate increases (chain length decreases).^{29–31} It is not clear whether this increase is real or an artifact caused by various aspects of SEC measurement.

To explore the possible effect of these differences on the estimates for radical reactivity ratios, each data set (20 Hz/DRI, 20 Hz/LS, 50 Hz/DRI, 50 Hz/LS) was first considered separately. Monomer reactivity ratios were set to the values determined from composition experiments ($r_{ST} = 0.61$, $r_{BMA} = 0.42$), and $k_{111}(k_{p,BMA})$, $k_{222}(k_{p,ST})$, and radical reactivity ratios were fit by nonlinear regression of the data to the implicit penultimate model given by eqs 3 and 4. The resulting parameter estimates (with standard deviation) are summarized in Table 5, with the corresponding curves plotted against the experimental data in Figure 3a. The estimates for $k_{p,BMA}$ and $k_{p,ST}$ are close to the average of the two homopolymer repeats in each set. Although these end points vary, the shapes of the four curves are very similar. The estimates for s_{ST} vary between 0.31 and 0.35. For all cases s_{BMA} cannot be adequately estimated, as the standard deviation is larger than the parameter value. The inability to obtain good estimates for both radical reactivity ratios is not unusual, as discussed in previous literature.^{6,23} In addition, the small differences in estimated s values with detector type were also observed by Coote et al. for ST/MMA and attributed to amplification of small statistical differences between data sets.⁶

The four data sets at 70 °C are thus combined together for the purpose of estimating the unknown parameters. As summarized in Table 5, this global fit resulted in $k_{p,BMA}$ and $k_{p,ST}$ estimates that are in good agreement with the predictions from eqs 7 and 8 and an estimate of 0.32 for s_{ST} . (The value for s_{BMA} remains indeterminate.) A similar estimate ($s_{ST} = 0.36$) is obtained when $k_{p,BMA}$ and $k_{p,ST}$ are fixed at the IUPAC values. The latter fit is plotted against the combined data set in Figure 3b. Also shown in this figure is the $k_{p,copo}$ calculated using the

Table 5. Kinetic Coefficients Estimated from the Implicit Penultimate Model Fit to Experimental $k_{p,copo}$ Data Obtained at 70–120 °C

T (°C)	data set	data points	$k_{p,ST}$ (L mol ⁻¹ s ⁻¹)	$k_{p,BMA}$ (L mol ⁻¹ s ⁻¹)	s_{ST}	s_{BMA}
70	20 Hz, DRI	10	484 ± 34	1105 ± 81	0.321 ± 0.036	n.d. ^a
	20 Hz, LS	10	519 ± 21	1121 ± 46	0.316 ± 0.057	n.d.
	50 Hz, DRI	10	532 ± 20	1399 ± 57	0.341 ± 0.021	n.d.
	50 Hz, LS	10	541 ± 28	1395 ± 74	0.321 ± 0.026	n.d.
	all data	40	519 ± 28	1217 ± 69	0.322 ± 0.027	n.d.
	all data	40	480 ^b	1242 ^b	0.356 ± 0.018	n.d.
100	100 Hz, DRI and LS	22	1283 ± 28	2670 ± 60	0.386 ± 0.039	1.066 ± 0.634
	100 Hz, DRI and LS	22	1200 ^b	2367 ^b	0.449 ± 0.121	n.d.
120	50 and 100 Hz, DRI and LS	64	2017 ± 137	3251 ± 213	0.381 ± 0.095	1.023 ± 0.967
	50 and 100 Hz, DRI and LS	64	2044 ^b	3446 ^b	0.388 ± 0.077	0.771 ± 0.480
combined fit 70–120		126	IUPAC ^c	IUPAC ^c	0.435 ± 0.046	0.624 ± 0.197

^a Standard deviation is larger than the parameter estimate. ^b IUPAC benchmark value, as calculated by eqs 7 and 8. ^c Values at each temperature calculated by eqs 7 and 8.

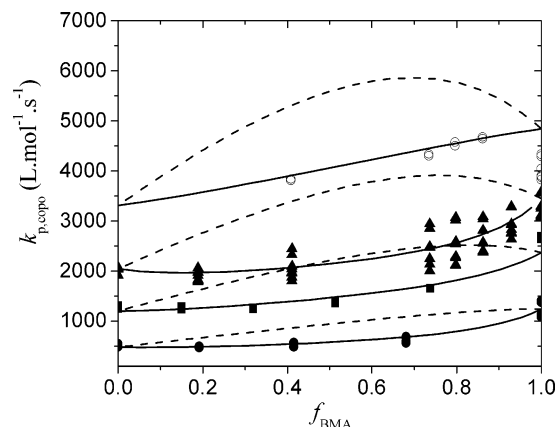


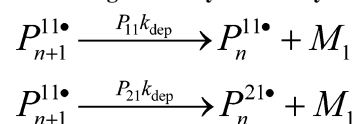
Figure 4. Experimental $k_{p,copo}$ data vs butyl methacrylate monomer mole fraction obtained by PLP/SEC at 70 (●), 100 (■), 120 (▲), and 140 °C (○). Terminal model predictions are indicated by dashed lines; penultimate model predictions calculated with $s_{ST} = 0.44$ and $s_{BMA} = 0.62$ are indicated by solid lines.

ST/BMA monomer and radical reactivity ratios from Davis et al.⁸ $r_{ST} = 0.72$, $r_{BMA} = 0.45$, $s_{ST} = 0.50$, $s_{BMA} = 0.67$. Although estimated from data at lower temperature (25 and 55 °C), these literature values provide a similar reasonable fit to the 70 °C data from Table 4. Also plotted in Figure 3b is the value of $k_{p,copo}$ calculated according to the terminal model (eq 2). As found by previous investigators,^{3,6,8} the terminal model significantly overpredicts experimental values for styrene/methacrylate copolymerization by as much as 70%.

With this confirmation of the experimental techniques and data treatment, we turn our focus to higher temperatures. Data were collected at 100, 120, and 140 °C in bulk monomer, with the resulting $k_{p,copo}$ values presented in Figure 4 as a function of f_{BMA} . At the higher temperatures, the MWDs begin to lose the characteristic PLP structure; however, all data retained in the set have a discernible secondary inflection point.²⁴ Possible explanations for the loss of structure include the influence of thermally generated styrene radicals and the influence of BMA depropagation, the latter effect discussed in more detail below. Despite the larger scatter at temperatures above 120 °C, a clear penultimate effect on $k_{p,copo}$ is observed, as seen by the poor fit by the terminal model.

Depropagation has a slight influence on observed BMA homopropagation kinetics at 140 °C, even at bulk monomer conditions.¹⁵ A k_p value of 4840 L mol⁻¹ s⁻¹ is calculated according to eq 8, while an effective value is estimated as 4300 L mol⁻¹ s⁻¹ according to $k_p^{eff} = k_p - k_{dep}/[M]$,¹⁵ with k_{dep} (s⁻¹) calculated according to the expression in ref 7. This effect is responsible for the difference between observed and predicted

Scheme 2. Lowry Case 1 Scheme To Describe the Depropagation of Monomer-1 (Butyl Methacrylate, M_1) from a Chain Radical Ending in a Butyl Methacrylate Diad P_{n+1}^{11} ^a



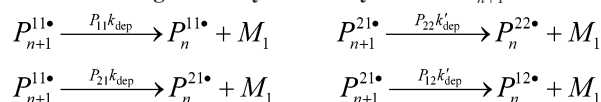
^a Probabilities P_{11} and P_{21} are introduced to track the identity of the penultimate unit resulting from the depropagation event.

k_p values at 140 °C seen in Figure 4 for $f_{BMA} = 1$. Thus, only the data at 70, 100, and 120 °C are used in the estimation of radical reactivity ratios. The results from the nonlinear parameter estimation at these temperatures are summarized as part of Table 5. Using IUPAC values for homopropagation rate coefficients, s_{ST} is estimated as 0.36 ± 0.02 at 70 °C, 0.45 ± 0.12 at 100 °C, and 0.39 ± 0.08 at 120 °C. With no discernible temperature effect, the data sets at 70, 100, and 120 °C are combined together. With this larger data set, the final estimate for s_{ST} is 0.44 ± 0.05 , and s_{BMA} is estimated as 0.62 ± 0.20 . These final values are remarkably close to those ($s_{ST} = 0.50$, $s_{BMA} = 0.67$) reported by Davis et al.⁸ and provide a reasonable representation of the complete data set between 70 and 140 °C, as shown in Figure 4.

These data show conclusively that penultimate effects are as important at higher temperatures as they are below 60 °C. They also provide some insight as to the origin of the penultimate effect. The lack of a discernible temperature dependency over this large temperature range suggests that the effect is largely entropic in nature, and thus is mainly captured in the frequency factor, as proposed by Heuts et al.³² However, a small temperature dependency may be hidden within the experimental scatter.

Depropagation Kinetics. While styrene has no appreciable depropagation rate at temperatures below 200 °C, methacrylates begin to depropagate under starved feed conditions ($[M] < 1$ mol L⁻¹) at temperatures greater than 120 °C.¹ Thus, only one monomer depropagates for the copolymerization in the temperature range of interest, the system first examined by Lowry.¹⁶ What is not clear for the system is the effect of the penultimate unit on depropagation. Lowry case 1, shown as Scheme 2, assumes that depropagation only happens to a methacrylate radical with another methacrylate unit present in the penultimate position. To combine this depropagation with penultimate propagation kinetics, it is also necessary to track whether the depropagation (with rate coefficient k_{dep}) leads to a formation of a $P_n^{11\bullet}$ or a $P_n^{21\bullet}$ radical, as these have different propagation rates according to penultimate kinetics (Scheme 1, with M_1 representing BMA). The relative formation of the two radical types is tracked by introducing P_{ij} as the probability of having

Scheme 3. Modified Scheme To Describe the Depropagation of Monomer-1 (Butyl Methacrylate, M_1) from a Chain Radical Ending in a Butyl Methacrylate Unit $P_{n+1}^{1\bullet}$ ^a



^a Probabilities P_{ij} are introduced to track the identity of the penultimate unit resulting from the depropagation event.

Table 6. Polymer Composition Data for Low-Conversion Styrene (ST)/Butyl Methacrylate (BMA) Copolymerization at High Temperature and Low Total Monomer Concentration ($[M]_{\text{tot}}$) in *n*-Octyl Acetate Solvent: Mole Fraction BMA in Copolymer (F_{BMA}) vs Mole Fraction BMA in Monomer Mixture (f_{BMA})

T (°C)	f_{BMA}	F_{BMA}	$[M]_{\text{tot}}$ (mol/L)	conv (%)
160–170	0.323	0.327	0.698	10.0
160–170	0.517	0.449	0.653	3.9
160–170	0.741	0.558	0.608	2.3
160–170	0.781	0.59	0.708	2.1
160–170	0.811	0.613	0.804	1.7
180–184	0.811	0.591	0.804	2.0
180–184	0.781	0.54	0.708	1.8
180–184	0.517	0.441	0.653	9.9
180–184	0.833	0.61	0.897	3.0
180–184	0.741	0.527	0.608	1.7
180–184	0.682	0.494	0.505	3.1
180–184	0.588	0.426	0.397	2.1
180–184	0.152	0.184	0.743	14.6
180–184	0.125	0.154	0.885	10.8
180–184	0.106	0.139	1.022	8.7
180–184	0.741	0.633	3.35	9.8
180–184	0.517	0.484	3.59	14.0
180–184	0.323	0.341	3.84	14.1
180–184	0.152	0.186	4.09	13.8

radical j with repeat unit i in the penultimate position such that ($P_{11} + P_{21}$) sums to unity. The equations to calculate these probabilities are described in our previous work.¹⁹

As discussed earlier, Lowry case 1 has been successfully applied to a variety of copolymerization systems with only one monomer depropagating. However, in the case of BMA/ST copolymerization, it may be that the methacrylate radical at the chain end will also depropagate with styrene in the penultimate position, as the resulting styrene radical would be resonance stabilized. This mechanism, here called “modified depropagation”, is shown in Scheme 3, where k'_{dep} represents the depropagation rate coefficient for radical $P_n^{2\bullet}$. The equations that combine the depropagation of Scheme 3 with the penultimate chain growth kinetics of Scheme 1 have also been derived.¹⁹

Simulations predict clear differences in BMA/ST copolymer composition and $k_{\text{p,copo}}$ curves when penultimate chain growth kinetics are combined with Lowry case 1 (Scheme 2) compared with modified depropagation (Scheme 3).¹⁹ However, these differences manifest themselves only at high temperatures (> 140 °C) and low monomer concentrations (< 1 mol L⁻¹), systems that are difficult to study under controlled kinetic conditions. Depropagation itself leads to broadening of the MWD and loss of PLP structure, as shown in recent work by Szablan et al.³³ Thus, attempts to obtain reliable $k_{\text{p,copo}}$ data using the PLP/SEC technique under these conditions were not successful.²⁴ However, several low-conversion copolymer composition experiments were performed with $[M]_{\text{tot}}$ below 1 mol L⁻¹ in *n*-octyl acetate and reaction temperature above 160 °C, as summarized in Table 6. Because of difficulties maintaining constant temperature during the experiments, a temperature range is reported for these data. The previous lower temperature results (Figure 1) indicate that this solvent has no observable effect on polymer

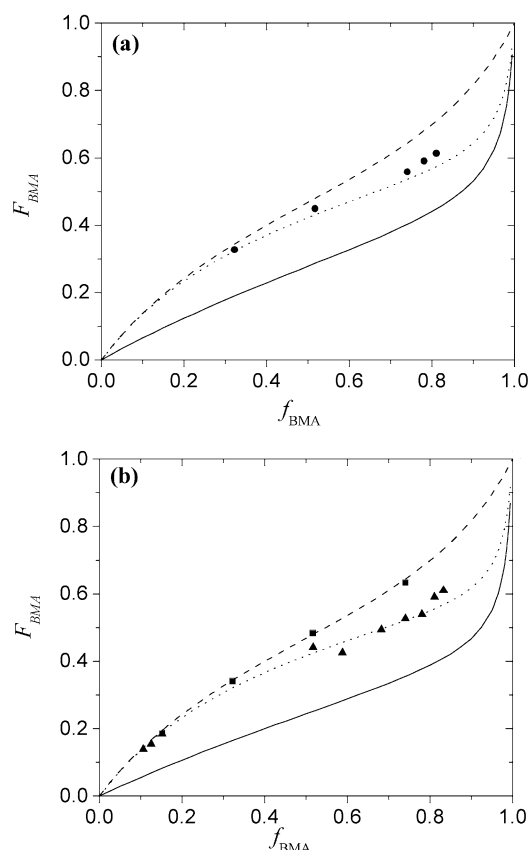


Figure 5. Experimental data for styrene/butyl methacrylate (BMA) copolymer composition vs BMA monomer mole fraction for polymer produced at (a) 165 °C with $[M]_{\text{tot}} = 0.7$ mol/L (●) and (b) 182 °C with $[M]_{\text{tot}} = 0.9$ mol/L (▲) and 182 °C with $[M]_{\text{tot}} = 3.5$ mol/L (■). Curves indicate predictions calculated assuming Mayo–Lewis (no depropagation) kinetics (—), Lowry case 1 depropagation combined with penultimate kinetics (···), and modified depropagation model combined with penultimate kinetics (—).

composition; thus, any deviation from the Mayo–Lewis behavior can be attributed to depropagation. As shown in the table, BMA compositions in the copolymer at 180 °C are always lower than the corresponding ones at 160 °C for low monomer concentrations and become higher when $[M]_{\text{tot}}$ increases.

To better understand how depropagation affects the compositions, experimental copolymer composition results are plotted against model predictions in Figure 5. The model curves were generated with the expressions derived previously,¹⁹ with $[M]_{\text{tot}} = 0.7$ mol L⁻¹ at 165 °C (Figure 5a) and $[M]_{\text{tot}} = 0.9$ mol L⁻¹ at 182 °C (Figure 5b), monomer and radical reactivity ratios as determined in this study, IUPAC homopropagation rate coefficients (eqs 7 and 8), and k_{dep} for BMA of 10 037 s⁻¹ at 165 °C and 21 580 s⁻¹ at 182 °C.⁷ For the modified depropagation model, k'_{dep} is assumed equal to k_{dep} , and for the Mayo–Lewis (no depropagation) case, k_{dep} is set to zero. In Figure 5b, the composition data at $[M]_{\text{tot}} > 3$ mol/L shows no or limited depropagation, which agrees well with the previous conclusions that depropagation becomes more important at lower $[M]_{\text{tot}}$.^{7,19} The predictions from the Lowry case 1 model at low monomer concentration best match the experimental composition data, which show significant deviation from the Mayo–Lewis plot at BMA monomer fractions larger than 50%. The modified depropagation model predicts significantly lower values for F_{BMA} than measured experimentally; thus, there is no evidence to suggest that BMA can depropagate from chain ends with styrene in the penultimate position.

Conclusions

The chain-growth copolymerization kinetics of ST and BMA have been studied over an extended temperature range, including industrially relevant high temperatures ($>120\text{ }^{\circ}\text{C}$) at which depropagation plays a role under starved-feed conditions. Low conversion experiments indicate that there is no observable temperature or solvent effect on the monomer reactivity ratios in the temperature range of $50\text{--}150\text{ }^{\circ}\text{C}$. Penultimate propagation kinetics have a strong effect on $k_{p,\text{copo}}$, the copolymer-averaged propagation kinetic rate coefficient measured by PLP combined with dual detector SEC analysis, over the complete temperature range examined. The combined composition and $k_{p,\text{copo}}$ data are well-represented by the implicit penultimate unit model. The experimental $k_{p,\text{copo}}$ data, the first in the literature demonstrating a strong penultimate effect at elevated temperatures, are adequately fit by temperature-independent radical reactivity ratios, suggesting a strong entropic contribution to penultimate chain-growth kinetics.

Depropagation has an observable effect on polymer composition for ST/BMA copolymer produced at high temperatures and low monomer concentrations. Attempts to measure $k_{p,\text{copo}}$ data at similar conditions proved unsuccessful. However, the composition data are sufficient to conclude that the Lowry case 1 model of depropagation well describes the polymerization system. These kinetic studies provide a sound basis for the fundamental modeling of styrene/methacrylate free-radical copolymerization under industrially relevant starved-feed conditions, to be combined with our previous methacrylate/acrylate study⁷ to formulate a full terpolymerization model.

Acknowledgment. We thank E. I. du Pont de Nemours and Co. and the Natural Sciences and Engineering Research Council of Canada for financial support of this work and Mr. Moritz Gadermann and Dr. Sabine Beuermann of Göttingen University for helpful discussions regarding depropagation mechanisms.

References and Notes

- (1) Grady, M. C.; Simonsick, W. J., Jr.; Hutchinson, R. A. *Macromol. Symp.* **2002**, *182*, 149–168.
- (2) Mayo, F. R.; Lewis, F. M. *J. Am. Chem. Soc.* **1944**, *66*, 1594–1601.
- (3) Fukuda, T.; Ma, Y.; Inagaki, H. *Macromolecules* **1985**, *18*, 17–26.
- (4) Davis, T. P.; O'Driscoll, K. F.; Piton, M. C.; Winnik, M. A. *J. Polym. Sci., Part C: Polym. Lett.* **1989**, *27*, 181–185.
- (5) Coote, M. L.; Zammit, M. D.; Davis, T. P.; Willett, G. D. *Macromolecules* **1997**, *30*, 8182–8190.
- (6) Coote, M. L.; Johnston, L. P. M.; Davis, T. P. *Macromolecules* **1997**, *30*, 8191–8204.
- (7) Li, D.; Grady, M. C.; Hutchinson, R. A. *Ind. Eng. Chem. Res.* **2005**, *44*, 2506–2517.
- (8) Davis, T. P.; O'Driscoll, K. F.; Piton, M. C.; Winnik, M. A. *Macromolecules* **1990**, *23*, 2113–2119.
- (9) Stergiou, G.; Dousikos, P.; Pitsikalis, M. *Eur. Polym. J.* **2002**, *38*, 1963–1970.
- (10) Otsu, T.; Ito, T.; Imoto, M. *Kogyo Kagaku Zasshi* **1966**, *69*, 986–990.
- (11) Luskin, L. S.; Myers, R. J. *Encycl. Polym. Sci. Technol.* **1964**, *1*, 246–328.
- (12) Simionescu, C. I.; Simionescu, B. C.; Ioan, S. *J. Macromol. Sci., Chem.* **1985**, *A22*, 765–778.
- (13) Beuermann, S.; Buback, M.; Isemer, C.; Wahl, A. *Proc. 6th Meeting Supercrit. Fluids Chem. Mater.* **1999**, 331–336.
- (14) Bywater, S. *Trans. Faraday Soc.* **1955**, *51*, 1267–1273.
- (15) Hutchinson, R. A.; Paquet, D. A., Jr.; Beuermann, S.; McMinn, J. H. *Ind. Eng. Chem. Res.* **1998**, *37*, 3567–3574.
- (16) Lowry, G. G. *J. Polym. Sci.* **1960**, *42*, 463–477.
- (17) Wittmer, P. *Adv. Chem. Ser.* **1971**, *99*, 140–174.
- (18) Kukulj, D.; Davis, T. P. *Macromolecules* **1998**, *31*, 5668–5680.
- (19) Li, D.; Leiza, J. R.; Hutchinson, R. A. *Macromol. Theory Simul.* **2005**, *14*, 554–559.
- (20) Reddy, G. V. R.; Joseph, V. S.; Mani, K. C. *J. Appl. Polym. Sci.* **2000**, *77*, 398–408.
- (21) Buback, M.; Gilbert, R. G.; Hutchinson, R. A.; Klumperman, B.; Kuchta, F.; Manders, B. G.; O'Driscoll, K. F.; Russell, G. T.; Schweer, J. *Macromol. Chem. Phys.* **1995**, *196*, 3267–3280.
- (22) Beuermann, S.; Buback, M.; Davis, T. P.; Gilbert, R. G.; Hutchinson, R. A.; Kajiwar, A.; Klumperman, B.; Russell, G. T. *Macromol. Chem. Phys.* **2000**, *201*, 1355–1364.
- (23) Hutchinson, R. A.; McMinn, J. H.; Paquet, D. A., Jr.; Beuermann, S.; Jackson, C. *Ind. Eng. Chem. Res.* **1997**, *36*, 1103–1113.
- (24) Li, N. MSc Thesis, Queen's University, Kingston, ON, 2005.
- (25) Zhang, M.; Ray, W. H. *J. Appl. Polym. Sci.* **2002**, *86*, 1630–1662.
- (26) *Polymer Handbook*, 4th ed.; Brandrup, J., Immergut, E. H., Grulke, E. A., Eds.; Wiley-Interscience: New York, 1999.
- (27) Hutchinson, R. A.; Paquet, D. A., Jr.; McMinn, J. H.; Beuermann, S.; Fuller, R. E.; Jackson, C. *5th International Workshop on Polymer Reaction Engineering*; DECHEMA Monographs 131; VCH Publishers: Weinheim, Germany, 1995; pp 467–492.
- (28) Hutchinson, R. A.; Beuermann, S.; Paquet, D. A., Jr.; McMinn, J. H. *Macromolecules* **1997**, *30*, 3490–3493.
- (29) Beuermann, S. *Macromolecules* **2002**, *35*, 9300–9305.
- (30) Willemse, R. X. E.; Stall, B. P. P.; van Herk, A. M.; Pierik, S. C. J.; Klumperman, B. *Macromolecules* **2003**, *36*, 9797–9803.
- (31) Olaj, O. F.; Zoder, M.; Vana, P.; Kornherr, A.; Schnöll-Bitai, I.; Zifferer, G. *Macromolecules* **2005**, *38*, 1944–1948.
- (32) Heuts, J. P. A.; Gilbert, R. G.; Maxwell, I. A. *Macromolecules* **1997**, *30*, 726–736.
- (33) Szablan, Z.; Stenzel, M. H.; Davis, T. P.; Barner, L.; Barner-Kowollik, C. *Macromolecules* **2005**, *38*, 5944–5954.

MA060411L